

1           **Extensive genetic diversity among populations of the malaria**  
2           **mosquito *Anopheles moucheti* revealed by population genomics**

3   Caroline Fouet<sup>1\*</sup>, Colince Kamdem<sup>1</sup>, Stephanie Gamez<sup>1</sup>, Bradley J. White<sup>1,2\*</sup>

4   <sup>1</sup>Department of Entomology, University of California, Riverside, CA 92521

5   <sup>2</sup>Center for Disease Vector Research, Institute for Integrative Genome Biology,

6   University of California, Riverside, CA 92521

7   \*Corresponding authors: [caroline.fouet@ucr.edu](mailto:caroline.fouet@ucr.edu); [bwhite@ucr.edu](mailto:bwhite@ucr.edu)

8

9

10   **Key words:** *Anopheles moucheti*, population genomics, RADseq, *de novo* assembly

11 **Abstract**

12 **Background:** Recent intensive efforts to control malaria in African countries expose  
13 vector populations to additional adaptive challenges. The main malaria mosquitoes  
14 of the continent display an array of adaptive strategies to cope with such challenges.  
15 The development of genomic resources will empower genetic studies that are  
16 crucial to understand the evolutionary history and adaptive potential of these  
17 vectors.

18 **Methodology/Principal findings:** Here we constructed double-digest Restriction  
19 Associated DNA (ddRAD) libraries and generated 6461 Single Nucleotide  
20 Polymorphisms (SNPs) that we used to explore the population structure and  
21 demographic history of wild-caught *Anopheles moucheti* from Cameroon. The  
22 genome-wide distribution of allelic frequencies among sampled populations best  
23 fitted that of an old population at equilibrium, characterized by a weak genetic  
24 structure and extensive genetic diversity, presumably due to a large long term  
25 effective population size. In contrast to other important African malaria vectors,  
26 polymorphic chromosomal inversions play little role in the genome architecture and  
27 evolutionary adaptation of *An. moucheti*.

28 **Conclusions/Significance:** Our study provides the first investigation of the genetic  
29 structure and diversity in *An. moucheti* at the genomic scale. Despite a weak genetic  
30 structure and absence of adaptive divergence, the adaptive potential of this  
31 mosquito remains significant owing to a great diversity and standing genetic  
32 variation that can be used to face current vector control measures and other rapid  
33 anthropogenic and environmental changes.

## 34 **Background**

35 *An. moucheti sensu lato* is a group of three related mosquito species (*An. moucheti*  
36 *moucheti*, *An. moucheti nigeriensis*, and *An. moucheti bervoetsi*) distributed across  
37 forested areas in Sub-Saharan Africa and distinguishable from each other by slight  
38 morphological differences [1]. The nominal species *An. moucheti moucheti*  
39 (hereafter *An. moucheti*) is the most widespread and one of the leading malaria  
40 vectors in the equatorial region [2–4]. The species breeds in slow moving streams  
41 and rivers close to villages where it contributes to high malaria transmission and  
42 often outcompete other main malaria vectors species. Despite this epidemiological  
43 significance, the evolutionary history and the evolvability of this mosquito remain  
44 understudied. Early investigations of the genetic structure based on allozymes and  
45 microsatellites detected no significant differentiation among *An. moucheti*  
46 populations over substantial geographic areas. This finding was particularly  
47 intriguing given the widespread distribution of *An. moucheti* in the evergreen forest  
48 areas of Central Africa. Moreover, African anopheline mosquito populations are  
49 increasingly exposed to intense selective pressure associated with the use of  
50 insecticides and insecticide-impregnated materials associated with recent expansive  
51 malaria control campaigns [5]. Such pressures are strong driving forces that often  
52 contribute to rapid diversification of vector populations at the scales of a few  
53 decades [6–8]. As a result, a more detailed characterization of the genomic  
54 architecture of *An. moucheti* will be crucial to: (1) understand the genetic bases  
55 allowing populations of this species to adapt to such a wide geographic area and (2)

56 predict the evolutionary potential of this vector in face of selective constraints  
57 imposed by rapidly changing environments.

58

59 Thanks to recent progresses in sequencing technology, high-resolution sequence  
60 information can be generated for virtually any living organism. However, while  
61 significant progresses have been made in genomic studies of other African  
62 anopheline mosquitoes [9], *An. moucheti* has lagged behind mainly because of the  
63 absence of genomic resources. So far, this species crucially lacks a reference genome  
64 assembly, a physical or linkage map and laboratory strains that are essential to  
65 generate high-quality sequencing information and to enable robust interpretations  
66 of natural polymorphisms.

67

68 To start filling this gap, we have conducted the first screening of genetic variation  
69 across the genome of wild populations of *An. moucheti*. We have performed a high-  
70 throughput sequencing of reduced representation libraries in 87 wild-caught  
71 individuals from Cameroon and used a *de novo* assembly to identify thousands of  
72 RAD loci scattered throughout the genome. Using high-quality Single Nucleotide  
73 Polymorphisms (SNPs) identified within these loci, we have investigated the genetic  
74 relatedness and population history of our samples. We found that populations of *An.*  
75 *moucheti* are characterized by extensive gene flow and a great genetic diversity. This  
76 vector appears particularly adapted to challenge the selective pressures imposed by  
77 vector controls and rapid human-induced environmental modifications.

78

## 79 **Methods**

### 80 **Mosquito sampling and sequencing**

81 This study included two *An. moucheti* populations from the Cameroonian equatorial  
82 rainforest. A total of 98 mosquitoes (97 adults and 1 larva) were collected in August  
83 and November 2013 Olama and Nyabessan, respectively (Table 1). The two  
84 locations are separated by ~200 km (Fig. 1A) and are crossed respectively by the  
85 Nyong and the Ntem rivers that provide the breeding sites for *An. moucheti* larvae.  
86 Specimens were identified as *An. moucheti moucheti* using morphological  
87 identification keys and a diagnostic PCR [1,10,11]. We extracted genomic DNA of  
88 specimens using either the DNeasy Blood and Tissue kit (Qiagen) or the Zymo  
89 Research MinPrep kit. We used 10ul (~50ng) of genomic DNA to prepare double-  
90 digest Restriction-site Associated DNA libraries following a modified protocol of  
91 Peterson et al.,2012 [12]. *MluC1* and *NlaIII* restriction enzymes were used to digest  
92 DNA of individual mosquitoes yielding RAD-tags of different sizes to which short  
93 unique DNA sequences (barcodes) were ligated to enable the identification of reads  
94 belonging to each specimen. The digestion products were purified and pooled. DNA  
95 fragments with size ~400bp were selected and amplified via PCR. The distribution  
96 of fragment sizes was checked on a BioAnalyzer (Agilent Technologies, Inc., USA)  
97 before sequencing. The sequencing was performed on an Illumina HiSeq2000  
98 platform (Illumina Inc., USA) (Genomic Core Facility, University of California,  
99 Riverside) to yield single-end reads of 101 bp.

### 100 ***De novo* assembly and SNP discovery**

101 We used the bioinformatics pipeline Stacks v1.35 [13] to process Illumina short  
102 reads. The program *process\_radtags* was first used to sort the reads according to the  
103 barcodes and to trim all reads to 96-bp in length by removing index and barcode  
104 sequences from the ends of the reads. Reads with ambiguous barcodes, those that  
105 did not contain the *NlaIII* recognition site and those with low-quality scores  
106 (average Phred score < 33) were excluded. The program *ustacks* was then utilized  
107 for a *de novo* assembly enabling the identification of consensus RAD loci in each  
108 individual in our populations. We allowed a maximum of 2 nucleotide mismatches  
109 between stacks (M parameter in *ustacks*) and we required a minimum of three reads  
110 to create a stack (m parameter in *ustacks*). Using the *cstacks* program, a catalogue of  
111 loci was built to synchronize variations across all individuals in our populations.  
112 Finally, we utilized the *populations* program to calculate population genetic  
113 parameters and output SNPs in different formats. To avoid bias associated with less  
114 informative SNPs or possible false positive SNPs (due to sequencing or pipeline  
115 errors), only RAD loci scored in at least 70-80% of individuals were retained for  
116 further analyses.

### 117 **Population genomic analyses**

118 SNP files outputted by the *populations* program were used to assess the population  
119 genetic structure with a Principal Component Analysis (PCA) and a Neighbor-joining  
120 tree analysis using respectively the R packages *adegenet* and *ape* [14,15]. We also  
121 explored patterns of ancestry and admixture in *An. moucheti* individuals in  
122 ADMIXTURE v1.23 [16] with 10-fold cross-validation for k assumed ancestral  
123 populations (k= 1 through 6). The optimal number of clusters was confirmed using

124 the Discriminant Analysis of Principal Component (DAPC) method which explores  
125 the number of genetically distinct groups by running a k-means clustering  
126 sequentially with increasing numbers and by comparing different clustering  
127 solutions using Bayesian Information Criterion (BIC) [14]. We examined the  
128 population genetic diversity, conformity to Hardy-Weinberg equilibrium and  
129 demographic background using several statistics calculated with the *populations*  
130 program. Precisely, to assess the global genetic diversity per population, we  
131 calculated the overall nucleotide diversity ( $\pi$ ) and the frequency of polymorphic  
132 sites within population. To make inferences on the demographic history and to test  
133 for departures from Hardy-Weinberg equilibrium, we utilized the Allele frequency  
134 spectrum and the Wright's inbreeding coefficient ( $F_{IS}$ ). To quantify the geographic  
135 and genetic differentiation between allopatric populations, we estimated the  
136 genome-wide average  $F_{ST}$  [17] on 2000 randomly selected SNPs in Genodive v1.06  
137 [18]. We also conducted an hierarchical Analysis of Molecular Variance (AMOVA)  
138 [19] on the same SNP set to quantify the effects of the geographic origin on the  
139 genetic variance among individuals. The statistical significance of  $F_{ST}$  and AMOVA  
140 was assessed with 10000 permutations. Finally, to examine the genomic  
141 architecture divergence, we inspected the genome-wide distribution of locus-  
142 specific estimates of  $F_{ST}$ .

### 143 **Identification of polymorphic chromosomal inversions**

144 The neutral recombination rate is notoriously reduced in genomic regions bearing  
145 chromosomal inversions, which results in elevated linkage disequilibrium (LD) in  
146 those regions relative to the rest of the genome. Thus, assessing genome-wide

147 patterns of LD can reveal clusters of highly correlated SNPs (LD blocks)  
148 corresponding potentially to chromosomal inversions. The R package LDna [20]  
149 allow the examination of the distinct LD network clusters within the genome of  
150 nonmodel species without the need of a linkage map or reference genome. We  
151 calculated LD, estimated as the  $r^2$  correlation coefficient between all pairs of SNPs, in  
152 PLINK v1.09 [21]. To avoid spurious LD due to the strong correlation between SNPs  
153 located on the same RAD locus, we randomly selected only one SNP within each RAD  
154 locus resulting in a dataset of 1056 variants containing less than 10% missing data.  
155 LDna was then used to identify clusters of highly correlated SNPs that were  
156 interpreted in light of the population demographic history, the population genetic  
157 structure and previous cytological studies of *An. moucheti*.

158

## 159 **Results**

### 160 **De novo assembly**

161 In total, 518,218 unique 96-bp RAD loci were identified from *de novo* assembly of  
162 reads in 98 individuals. We retained 946 loci that were present in all sampled  
163 populations and in at least 75% of individuals in every population, and we identified  
164 3027 high-quality biallelic SNPs from these loci.

### 165 **Population genetic structure**

166 First, we tested for the presence of cryptic genetic subdivision within *An. moucheti*  
167 with PCA, NJ trees and the ADMIXTURE ancestry model. A NJ tree constructed from  
168 a matrix of Euclidian distance using allele frequencies at 3027 genome-wide SNPs  
169 showed a putative subdivision of *An. moucheti* populations in two genetic clusters  
170 (Fig. S1). The first three axes of PCA also revealed a number of outlier individuals  
171 separated from a main cluster (Fig. S1). However, when we ranked our sequenced  
172 individuals based on the number of sequencing reads, we noticed that one of the  
173 putative genetic clusters corresponded to a group of individuals having the lowest  
174 sequencing coverage. We excluded all these individuals and reduced our dataset to  
175 78 individuals. We conducted a *de novo* assembly and analyzed the relationship  
176 between the 78 remaining individuals at 6461 genome-wide SNPs using PCA, NJ  
177 trees and ADMIXTURE. Both the k-means clustering (DAPC) and the variation of the  
178 cross-validation error as a function of the number of ancestral populations in  
179 ADMIXTURE revealed that the polymorphism of *An. moucheti* resulted from only one  
180 ancestral population ( $k = 1$ ) (Fig. 1E,F). PCA and NJ depicted a homogeneous cluster  
181 comprising all 78 individuals providing additional evidence of the lack of genetic or

182 geographic structuring among populations. Unsurprisingly, the overall  $F_{ST}$  was  
183 remarkably low between populations from the two sampling locations Olama and  
184 Nyabessan ( $F_{ST} = 0.008$ ,  $p < 0.005$ ). Similarly, the distribution of  $F_{ST}$  values across the  
185 6461 SNPs showed a large dominance of very low  $F_{ST}$  values (Fig. 2). The highest per  
186 locus  $F_{ST}$  was only 0.126, while 5006 of the 6461 loci revealed  $F_{ST}$  near zero. The  
187 modest geographic differentiation was also well illustrated by a hierarchical  
188 AMOVA, which showed that the genetic variance was explained essentially by  
189 within-individual variations (99.7%). Finally, we found very low overall Wright's  
190 inbreeding coefficient ( $F_{IS} = 0.0014$  in Nyabessan and  $F_{IS} = 0.0025$  in Olama) (Table  
191 2) suggesting that allelic frequencies within both populations were in accordance  
192 with proportions expected under the Hardy-Weinberg equilibrium.

### 193 **Genetic diversity and demographic history**

194 The estimates of the overall nucleotide diversity ( $\pi = 0.0020$  and  $\pi = 0.0016$ ,  
195 respectively, in Olama and Nyabessan) (Table 2) were within the range of average  
196 values found in other African *Anopheles* species using RAD-seq approaches [8,22–  
197 24]. Notorious demographic expansions have been described in natural populations  
198 of this insect clade [25], and the values of  $\pi$  observed in *An. moucheti* likely reflect  
199 the level genetic diversity of a population with large effective size. The great genetic  
200 diversity of *An. moucheti* was also illustrated by the percentage of polymorphic sites.  
201 Of the 6461 variant sites, 89.60% were polymorphic in Olama and 34.82% in  
202 Nyabessan (Table 2). The difference observed between the two locations can be  
203 related to the sample size ( $n = 19$  in Nyabessan and  $n = 59$  in Olama) or to  
204 demographic particularities that persists between the two geographic sites despite a

205 massive gene flow. To infer the demographic history of *An. moucheti*, we examined  
206 the Allele Frequency Spectrum (AFS), summarized as the distribution of the major  
207 allele in one population. This approach represented a substitute to model-based  
208 methods that provide powerful examinations of the history of genetic diversity by  
209 modeling the AFS at genome-wide SNP variants, but that couldn't be implemented  
210 here due to the lack of reference genome assembly. The frequency distribution of  
211 the major allele  $p$  (Fig. 3) indicates that the majority of loci that are polymorphic  
212 between Olama and Nyabessan are fixed within each population as shown by the  
213 predominance of SNPs at frequencies equal to 1. Ranges of allele frequencies are  
214 similar in Olama and Nyabessan (between 0.47 and 1 in Olama and between 0.34  
215 and 1 in Nyabessan). These frequency ranges are expected for old populations at  
216 equilibrium capable of accumulating high amount of genetic diversity.

### 217 **Polymorphic chromosomal inversions**

218 LD analyses at 1056 highly filtered SNPs revealed a globally low LD in the *An.*  
219 *moucheti* genome (average genome-wide  $r^2 = 0.0149$ ) as expected in highly  
220 polymorphic populations with large effective size. We used LDna to cluster the LD  
221 values and to identify Single Outlier Clusters (SOC) that can be associated with  
222 distinct or multiple evolutionary phenomena in the *An. moucheti* history. Results  
223 showed the presence of two independent LD blocks in our samples (Fig. 4).  
224 Cytogenetic analyses have identified three polymorphic chromosomal inversions in  
225 Cameroon samples [26] and the two LD clusters could well correspond to linked  
226 SNPs within inversions. Studies on *Anopheles baimaii* [20] have shown that when  
227 SOC are generated by polymorphic inversions, SNPs within the SOC can clearly

228 separate the three expected karyotypes (inverted homozygotes, heterozygotes and  
229 uninverted homozygotes). We conducted downstream analyses with a PCA using  
230 respectively 30 and 34 SNPs identified within the two SOC. As shown on Fig,  
231 although individuals were spread along three PCA axes, no distinct cluster could be  
232 identified for the first SOC. likewise, except three outlier individuals, the second SOC  
233 formed a single genetic cluster (Fig. 4B,C). The two LD clusters were apparently not  
234 associated with polymorphic inversions, but caution must be used when  
235 interpreting this result as evidence of absence of inversions in our samples because  
236 other LDna analyses conducted on *An. funestus* and *An. gambiae* which contain tens  
237 of polymorphic inversions did not systematically identified the segregating  
238 karyotypes of key adaptive inversions (results not shown). However, based on our  
239 findings and previous cytogenetic studies, we can reasonably think that inversion  
240 polymorphisms are less important in the genome architecture *An. moucheti*  
241 compared with that of other important African malaria vectors such as *An. gambiae*  
242 and *An. funestus* whose populations often segregate along clines of multiple  
243 polymorphic inversions in nature.  
244

245 **Discussion**

246 We have analyzed genome-wide polymorphism and characterized some of the  
247 baseline population genomic parameters in *An. moucheti*, an important malaria  
248 vector in the African rainforest. We found very little differentiation among our  
249 samples, with most of the genetic variation distributed within individuals. Although  
250 a more substantial sampling will be necessary to fully appreciate the population  
251 genetic structure of this species, our sampling likely reflects the current dynamic of  
252 *An. moucheti* populations in Cameroon. It is worth mentioning that we have  
253 surveyed a total of 28 locations across the country, some of which were known from  
254 several past surveys to harbor *An. moucheti* populations [1–4,27,28], but we  
255 confirmed the presence of the species in only 2 villages. Extant populations of *An.*  
256 *moucheti* are distributed in patches of favorable habitats along river networks  
257 where larval populations breed. Our results indicate that despite this apparent  
258 fragmentation, connectivity and gene flow are high among population aggregates.  
259 The weak population genetic structure of *An. moucheti* observed with genome-wide  
260 markers corroborated results obtained with microsatellites and allozymes [2,3]. A  
261 survey of eight microsatellite loci revealed that the highest  $F_{ST}$  among Cameroonian  
262 populations was as low as 0.003. Nevertheless, a substantial differentiation was  
263 found between samples from different countries consistent with an isolation-by-  
264 distance model [3]. It is clear that a deep sequencing of continental populations is  
265 necessary to further clarify the status of these putative subpopulations that seem to  
266 be endemic to different countries. But, samples collected at lower spatial scales like  
267 ours are also relevant as they can allow robust inferences about ongoing selective

268 processes. We have found that signatures of selection are very rare in the genome of  
269 *An. moucheti* populations from the Cameroonian rainforest. Populations remain  
270 largely undifferentiated throughout the genome, with  $F_{ST}$  values near zero across the  
271 vast majority of segregating sites. Interestingly, polymorphic chromosomal  
272 inversions that are the prime source of adaptive polymorphisms in many other  
273 important malaria vectors seem to be less vital in the evolution of *An. moucheti*. The  
274 characterization of chromosomal inversions with cytogenetic methods can be  
275 laborious, particularly with regard to the identification of new inversions [26,29].  
276 We have implemented a recently designed method that used Next Generation  
277 Sequencing and LD estimates to identify paracentric inversions. Although the  
278 method holds great promise in identifying inversions in genomes of nonmodel  
279 species like *An. moucheti*, care should be taken when interpreting the results. So far,  
280 only three paracentric polymorphic inversions have been discovered in *An. moucheti*  
281 thanks to cytogenetics [26]. The ecological, behavioral or functional roles of these  
282 inversion polymorphisms remain unknown. In keeping with cytogenetic  
283 observations, LD analyses revealed the presence of only a few LD clusters that could  
284 not be unambiguously associated with inversions. On the other hand, the low overall  
285 LD observed across the genome reflected the significant genetic polymorphism that  
286 seems to prevail in *An. moucheti* populations. This polymorphism translates into  
287 exceptional levels of overall genetic diversity and very high percentage of  
288 polymorphic sites that are in the range of values found in other mosquito species  
289 undergoing a significant demographic expansion [8,24,25]. One of our main goals  
290 was to know if the genetic diversity of *An. moucheti* can provide cues about its

291 extensive spatial distribution and can help to predict its environmental resilience. In  
292 principle, evolutionary responses of species to human-induced or natural changes  
293 rely largely on available heritable variation, which reflects the evolutionary  
294 potential and adaptability to novel environments [30]. Therefore, the screening of  
295 genome-wide variation is supposed to be a sensible approach that may provide a  
296 generalized measure of evolutionary potential in species like *An. moucheti* for which  
297 direct ecological, evolutionary or functional tests are impossible [31]. Our  
298 population genomic analyses have depicted *An. moucheti* as a species with a great  
299 genetic diversity and consequently a sustainable long-term adaptive resilience.  
300 Implications of our findings in malaria epidemiology and control can be very  
301 significant. First, *An. moucheti* is essentially endophilic and is particularly sensitive  
302 to the principal measures currently employed to control malaria in Sub-Saharan  
303 Africa such as the massive use of Insecticide Treated Nets (ITNs) and Indoor  
304 Residual insecticide Spraying (IRS). For example, estimates of population effective  
305 size in one village in Equatorial Guinea indicated that both mass distribution of ITNs  
306 and IRS campaigns resulted in a decline of approximately 55% of *An. moucheti* [32].  
307 However, the great genetic diversity and the massive gene flow we observed within  
308 populations could easily enable *An. moucheti* to challenge population declines and  
309 recover from shallow bottlenecks. Moreover, most insecticide resistance  
310 mechanisms found in insects exploit standing genetic variation that allow to rapidly  
311 respond to the evolutionary challenge by increasing the frequency of existing  
312 variations rather than that of *de novo* mutations [33]. As a result, despite the current  
313 sensitivity of *An. moucheti* to common insecticides, the significant amount of

314 standing genetic variation provides the species with a great potential to challenge  
315 insecticides and other types of human-induced stress.

316

317 Recent advances in sequencing allow sensitive genomic data to be generated for  
318 virtually any species [30]. However, the most important information we can obtain  
319 from population resequencing approaches often depends on the availability and the  
320 quality of genomic resources such as a well-annotated reference genome.  
321 Nevertheless, the reduced genome sequencing strategy (RAD-seq) offers a cost-  
322 effective strategy that can be used to effectively study the genetic variation in a  
323 broad range of species from yeast to plants, insects, etc., in the absence of reference  
324 genome. We have extended this approach to the study of the genetic structure of an  
325 understudied epidemiologically important mosquito species. We have provided  
326 both significant baseline population genomic data and the methodological validation  
327 of one approach that should motivate further studies on this species and other  
328 understudied anopheline mosquitoes lacking genomic resources.

329

330 **Acknowledgements**

331 Funding for this project was provided by the University of California Riverside and  
332 NIH grants 1R01AI113248 and 1R21AI115271 to BJW. We thank populations and  
333 authorities of the locations surveyed for their kind collaboration.

334

335 **References**

- 336 1. Kengne P, Antonio-Nkondjio C, Awono-Ambene HP, Simard F, Awolola TS,  
337 Fontenille D. Molecular differentiation of three closely related members of the  
338 mosquito species complex, *Anopheles moucheti*, by mitochondrial and ribosomal  
339 DNA polymorphism. *Med. Vet. Entomol.* 2007;21:177–82.
- 340 2. Antonio-Nkondjio C, Simard F, Cohuet A, Fontenille D. Morphological variability in  
341 the malaria vector, *Anopheles moucheti*, is not indicative of speciation: evidences  
342 from sympatric south Cameroon populations. *Infect. Genet. Evol.* 2002;2:69–72.
- 343 3. Antonio-Nkondjio C, Ndo C, Kengne P, Mukwaya L, Awono-Ambene P, Fontenille  
344 D, et al. Population structure of the malaria vector *Anopheles moucheti* in the  
345 equatorial forest region of Africa. *Malar. J.* 2008;7:120.
- 346 4. Antonio-Nkondjio C, Ndo C, Costantini C, Awono-Ambene P, Fontenille D, Simard  
347 F. Distribution and larval habitat characterization of *Anopheles moucheti*,  
348 *Anopheles nili*, and other malaria vectors in river networks of southern Cameroon.  
349 *Acta Trop.* 2009;112:270–6.
- 350 5. Bowen HL. Impact of a mass media campaign on bed net use in Cameroon. *Malar.*  
351 *J. Malaria Journal*; 2013;12:36.
- 352 6. Norris LC, Main BJ, Lee Y, Collier TC, Fofana A, Cornel AJ, et al. Adaptive  
353 introgression in an African malaria mosquito coincident with the increased usage of  
354 insecticide-treated bed nets. *Proc. Natl. Acad. Sci.* 2015;201418892.
- 355 7. Clarkson CS, Weetman D, Essandoh J, Yawson AE, Maslen G, Manske M, et al.  
356 Adaptive introgression between *Anopheles* sibling species eliminates a major  
357 genomic island but not reproductive isolation. *Nat. Commun.* 2014;5:4248.

- 358 8. Kamdem C, Fouet C, Gamez S, White BJ. Pollutants and insecticides drive local  
359 adaptation in African malaria mosquitoes. *bioRxiv*. 2016;
- 360 9. Neafsey DE, Waterhouse RM, Abai MR, Aganezov SS, Alekseyev MA, Allen JE, et al.  
361 Highly evolvable malaria vectors: The genomes of 16 *Anopheles* mosquitoes. *Science*  
362 (80-. ). 2015;347:1258522–1258522.
- 363 10. Gillies MT, De Meillon B. *The Anophelinae of Africa South of the Sahara*. Second  
364 Edi. Johannesburg: Publications of the South African Institute for Medical Research;  
365 1968.
- 366 11. Gillies MT, Coetzee M. *A supplement to the Anophelinae of Africa south of the*  
367 *Sahara*. Johannesburg: The South African Institute for Medical Research; 1987.
- 368 12. Peterson BK, Weber JN, Kay EH, Fisher HS, Hoekstra HE. Double Digest RADseq:  
369 An Inexpensive Method for De Novo SNP Discovery and Genotyping in Model and  
370 Non-Model Species. *PLoS One*. 2012;7:e37135.
- 371 13. Catchen J, Hohenlohe P a., Bassham S, Amores A, Cresko W. Stacks: An analysis  
372 tool set for population genomics. *Mol. Ecol*. 2013;22:3124–40.
- 373 14. Jombart T. adegenet: a R package for the multivariate analysis of genetic  
374 markers. *Bioinformatics*. 2008;24:1403–5.
- 375 15. Paradis E, Claude J, Strimmer K. *Analyses of Phylogenetics and Evolution in R*  
376 *language*. *Bioinformatics*. 2004;20:289–90.
- 377 16. Alexander DH, Novembre J, Lange K. Fast model-based estimation of ancestry in  
378 unrelated individuals. *Genome Res*. 2009;19:1655–64.
- 379 17. Weir BS, Cockerham CC. Estimating F-statistics for the analysis of population  
380 structure. *Evolution (N. Y)*. 1984;38:1358–70.

- 381 18. Meirmans P, Van Tienderen P. GENOTYPE and GENODIVE: two programs for the  
382 analysis of genetic diversity of asexual organisms. *Mol. Ecol. Notes*. 2004;4:792–4.
- 383 19. Excoffier L, Smouse PE, Quattro JM. Analysis of molecular variance inferred from  
384 metric distances among DNA haplotypes: Application to human mitochondrial DNA  
385 restriction data. *Genetics*. 1992;131:479–91.
- 386 20. Kemppainen P, Knight CG, Sarma DK, Hlaing T, Prakash A, Maung Maung YN, et  
387 al. Linkage disequilibrium network analysis (LDna) gives a global view of  
388 chromosomal inversions, local adaptation and geographic structure. *Mol. Ecol.*  
389 *Resour.* 2015;n/a – n/a.
- 390 21. Purcell S, Neale B, Todd-Brown K, Thomas L, Ferreira M, Bender D, et al. PLINK:  
391 a toolset for whole-genome association and population-based linkage analysis. *Am. J.*  
392 *Hum. Genet.* 2007;81.
- 393 22. O’Loughlin SM, Magesa S, Mbogo C, Mosha F, Midega J, Lomas S, et al. Genomic  
394 Analyses of Three Malaria Vectors Reveals Extensive Shared Polymorphism but  
395 Contrasting Population Histories. *Mol. Biol. Evol.* 2014;1–14.
- 396 23. Kamdem C, Fouet C, Gamez S, White BJ. Genomic signatures of introgression at  
397 late stages of speciation in a malaria mosquito. *bioRxiv*. 2016;
- 398 24. Fouet C, Kamdem C, White BJ. Chromosomal inversions facilitate chromosome-  
399 scale evolution in *Anopheles funestus*. *bioRxiv*. 2016;
- 400 25. Donnelly MJ, Licht MC, Lehmann T. Evidence for recent population expansion in  
401 the evolutionary history of the malaria vectors *Anopheles arabiensis* and *Anopheles*  
402 *gambiae*. *Mol. Biol. Evol.* 2001;18:1353–64.
- 403 26. Sharakhova M V., Antonio-Nkondjio C, Xia a., Ndo C, Awono-Ambene P, Simard F,

404 et al. Polymorphic chromosomal inversions in *Anopheles moucheti*, a major malaria  
405 vector in Central Africa. *Med. Vet. Entomol.* 2014;28:337–40.

406 27. Antonio-Nkondjio C, Keraf CH, Simard F, Awono-Ambene P, Chouaibou M,  
407 Tchuinkam T, et al. Complexity of the malaria vectorial system in Cameroon:  
408 contribution of secondary vectors to malaria transmission. *J. Med. Entomol.*  
409 2006;43:1215–21.

410 28. Antonio-Nkondjio C, Demanou M, Etang J, Bouchite B. Impact of cyfluthrin  
411 (Solfac EW050) impregnated bed nets on malaria transmission in the city of  
412 Mbandjock : lessons for the nationwide distribution of long-lasting insecticidal nets  
413 (LLINs) in Cameroon. *Parasit. Vectors. Parasites & Vectors*; 2013;6:10.

414 29. Kirkpatrick M. How and why chromosome inversions evolve. *PLoS Biol.* 2010;8.

415 30. Ellegren H. Genome sequencing and population genomics in non-model  
416 organisms. *Trends Ecol. Evol. Elsevier Ltd*; 2014;29:51–63.

417 31. Harrisson K a., Pavlova A, Telonis-Scott M, Sunnucks P. Using genomics to  
418 characterize evolutionary potential for conservation of wild populations. *Evol. Appl.*  
419 2014;n/a – n/a.

420 32. Athrey G, Hodges TK, Reddy MR, Overgaard HJ, Matias A, Ridl FC, et al. The  
421 effective population size of malaria mosquitoes: large impact of vector control. *PLoS*  
422 *Genet.* 2012;8:e1003097.

423 33. Messer PW, Petrov D. Population genomics of rapid adaptation by soft selective  
424 sweeps. *Trends Ecol. Evol. Elsevier Ltd*; 2013;28:659–69.

425

426 **Author contributions**

427 Conceived and designed the experiments: CF CK BJW. Performed the experiments:

428 CF CK SG BJW. Analyzed the data: CF CK BJW. Wrote the paper: CF CK BJW.

429

430 **Competing interests**

431 The authors declare that they have no competing interests.

432 **Tables**

433 **Table 1:** Information on *An. moucheti* samples included in this study.

Sampling locations	Geographic coordinates	Sampling methods			Total
		HLC-OUT	HLC-IN	LC	
Nyabessan	2°24'00"N, 10°24'00"E	21	15	1	37
Olama	3°26'00"N, 11°17'00"E	30	31	0	61
Total					98

HLC-OUT, human landing catches performed outdoor; HLC-IN, human landing catches performed indoor; LC, larval collection

434

435 **Table 2:** Population genomic parameters based on 6461 variant sites reflecting the  
436 genetic diversity and conformity to Hardy-Weingberg equilibrium.

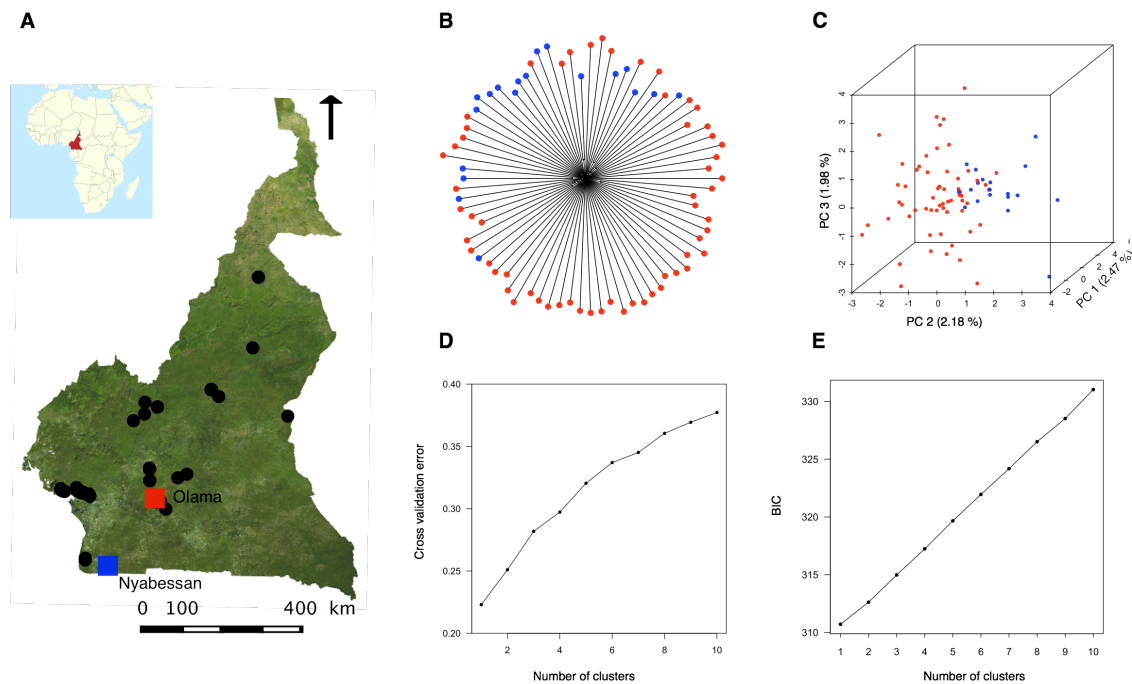
	n	Sites	Observed heterozygosity	$F_{IS}$	$\pi$	% polymorphic sites
<b>Variant positions</b>						
<b>Olama</b>	54.12	6 461	0.0445	0.0631	0.0505	89.60
<b>Nyabessan</b>	16.78	6 461	0.0334	0.0372	0.0402	34.82
<b>All positions</b>						
<b>Olama</b>	54.47	165 975	0.0017	0.0025	0.0020	3.49
<b>Nyabessan</b>	16.86	165 975	0.0013	0.0014	0.0016	1.36

437 **Figures**

438

439 **Figure 1:** Relationship between *An. moucheti* individuals from Olama and  
440 Nyabessan. (A) Map of the study site showing both the locations surveyed (small  
441 black dots) and the two villages (large red and blue squares) where *An. moucheti*  
442 samples were collected. (B) and (C) Absence of genetic structure within populations  
443 illustrated by neighbor-joining and PCA. The percentage of variance explained by  
444 each PCA axis is indicated. (D) and (E) Plots of the ADMIXTURE cross-validation  
445 error and the Bayesian Information Criterion (BIC) (DAPC) as a function of the  
446 number of genetic clusters indicating that  $k = 1$ . The lowest BIC and CV error  
447 indicate the suggested number of clusters.

448

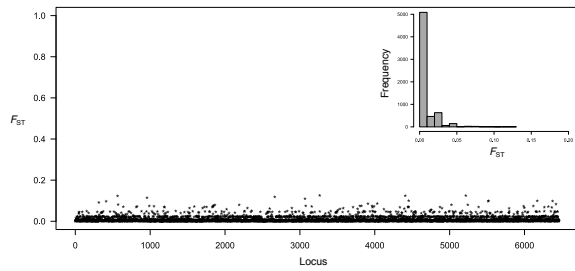


449

450 **Figure 2:** Frequency distribution of  $F_{ST}$  between Olama and Nyabessan across 6461

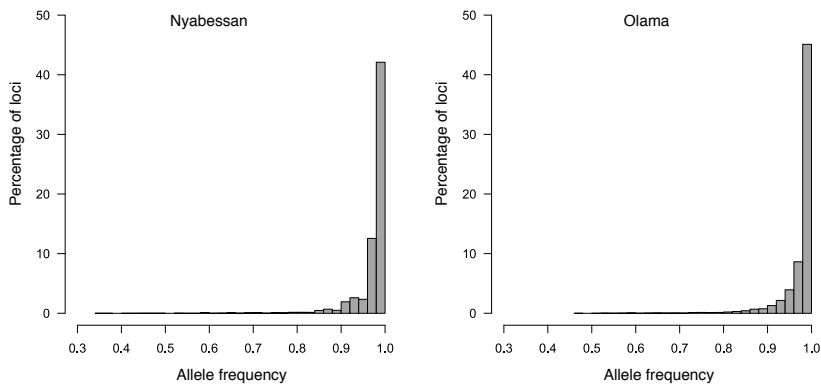
451 SNP loci and plot of these  $F_{ST}$  values along arbitrary positions in the genome.

452



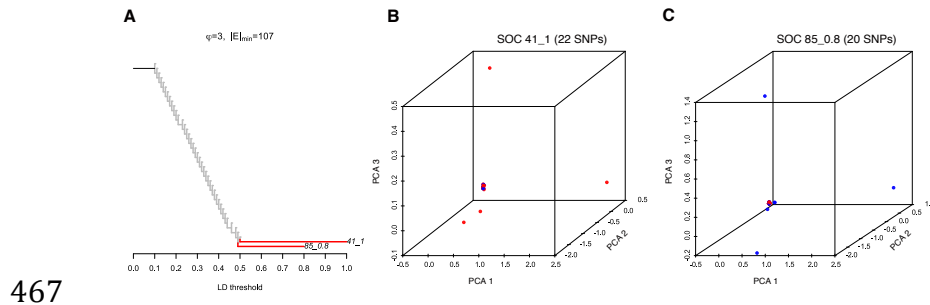
453

454 **Figure 3:** Allele Frequency Spectrum for 6461 SNP loci in Nyabessan and Olama  
455 populations. The x-axis presents the frequency of the major allele and the y-axis the  
456 frequency distribution of loci in each class of the major allele frequency.  
457



458

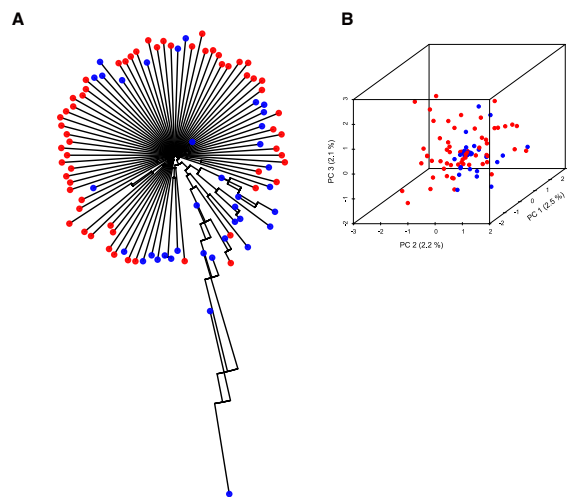
459 **Figure 4:** LDna analyses on 1056 SNPs showing the presence of two Single Outlier  
460 Clusters (SOCs) of linkage disequilibrium in *An. moucheti*. (A) Graph presenting the  
461 results obtained with values of the two parameters:  $\varphi$  (which controls when clusters  
462 are defined as outliers) and  $|E|_{\min}$ , the minimum number of edges required for a LD  
463 cluster to be considered as an outlier, indicated on top. LD thresholds are shown on  
464 the x-axis. (B) and (C) PCA indicating the population genetic structure inferred from  
465 SNPs within the two SOC (red: Olama; blue: Nyabessan).  
466



468 **Supplemental Material**

469 **Figure S1:** Selection of individuals included in final analyses based on the average  
470 per individual sequencing coverage. (A) and (B) Neighbor-joining tree and PCA  
471 indicating spurious population structure due to individuals with low sequencing  
472 coverage in Olama (red) and Nyabessan (blue).

473



474

475